Investigation of the dispersion of heavy-particle pairs and Richardson's law using kinematic simulation

A. ElMaihy and F. Nicolleau*
Mechanical Engineering, The University of Sheffield, Mapping Street, Sheffield, S1 3JD, United Kingdom
(Received 25 September 2004; revised manuscript received 11 January 2005; published 28 April 2005)

In this paper we investigate the dispersion of heavy-particle pairs (particles with inertia in a gravity field). We vary the particles' inertia when there is no gravity, and the particles' drift at constant inertia. We use kinematic simulation (KS) for which large values of the Reynolds number can be achieved. We investigate the pair diffusivity to discuss Richardson's law, and the locality-in-scale hypothesis that underlies that law, for different particle drifts and Stokes numbers. The effect of inertia and gravity on Richardson's law and the autocorrelation in time of the pair's separation are studied for an inertial scale ratio of 1000 and different initial separations Δ_0. We extend results from F. Nicolleau and J. C. Vassilicos, Phys. Rev. Lett. **90**, 024503 (2003) to three-dimensional (3D) KS and the diffusivity-based analysis of F. Nicolleau and G. Yu, Phys. Fluids **16**, 2309 (2004) to particles with inertia and gravity. We find that inertia impedes the locality-in-scale hypothesis whereas gravity improves it. However, the overall effect of gravity and inertia is to decrease the pair's diffusivity in the inertial range.

DOI: 10.1103/PhysRevE.71.046307 PACS number(s): 47.27.Qb, 47.27.Eq, 47.27.Gs, 47.27.Jv

I. INTRODUCTION

A. Introduction to heavy particles

One of the most important statistics of two-particle dispersion is the mean distance between the two particles. In particular, for a linear source it is the only two-particle statistics needed to calculate concentration fluctuations [1]. The calculation of concentration fluctuations is important for the prediction of reaction rates in chemical reactors and in the atmosphere because chemical reaction rates depend on the concentration covariance rather than on the average concentration. The calculation of concentration fluctuations is also important for air-quality control, combustion, and pollutant dispersal in geophysical flows [2].

In this paper we investigate the mean square distance between two heavy particles using kinematic simulation (KS). The KS code we use is based on [3,4].

The dynamic response of a heavy particle to a turbulent flow is different from that of a fluid element because of the particle's inertia and the body forces acting on the particle, typically gravity. The latter gives the heavy particle a finite drift velocity relative to the mean motion of the surrounding fluid. Therefore, tracking heavy particles is a more complex problem than the diffusion of fluid packets, gases, or small light particles. The dispersion of heavy particles in turbulent flows is characterised by both the properties of the particles and the properties of the turbulent flow that carries the particles. Particles can be characterized by their density, ρ_p, and their response time, τ_a.

The paper is organized as follows: in Sec. I we introduce the equations of motion and the kinematic simulation method we use. In Sec. II we introduce results and definitions for fluid particles. In Sec. III we introduce results and definitions for heavy particle dispersion. Section IV deals with the sole effect of inertia when the gravity is set to 0. In Sec. V we study the effect of only varying the drift parameter γ. In Sec. VI we consider the effect of initial separation, inertia and gravity on the particle-pair's memory. In Sec. VII the effect of inertia and gravity on the particle-pair's PDF is investigated. We conclude the paper in Sec. VIII.

B. Simplified equation of motion for heavy particles

The general equations of motion for heavy particles and how KS can be used to model heavy particles is discussed in [5,6].

In this paper we consider the motion of heavy spherical particles in a uniform, isotropic and stationary turbulent flow in which the fluid has a constant mean velocity (for sake of simplicity, taken to be zero).

We assume that the particles are much denser than the fluid and that the concentration of particles is small enough for the interaction between them to be neglected.

The forces acting on the particle should include: Stokes drag, virtual mass, pressure gradient, Basset history, and gravity. But we consider particles heavy enough (typically, $\rho_p/\rho_f \gg 1000$) for the pressure gradient, virtual mass, and Basset history terms to be neglected.

The particle is assumed to be small in comparison to the Kolmogorov microscale of turbulence and it is assumed that the presence of the particles does not modify the turbulence Eulerian velocity field.

The particle is considered to be much larger than the fluid molecules and to have an aerodynamic response time much larger than the mean molecular collision time so that the effect of Brownian motion can be neglected in comparison to the dispersion due to turbulence eddies.

Under these simplifying assumptions there are two forces acting on the particle which need to be retained: the fluid drag force produced by the motion of the particle relative to the surrounding fluid

*Eelctronic address: F.Nicolleau@Sheffield.ac.uk

$$-6\pi a\mu(\mathbf{V}-\mathbf{u})$$

and the force due to gravity

$$m_p\mathbf{g}.$$

The equation of motion for the heavy particle can then be written as

$$m_p\frac{d\mathbf{V}}{dt}=m_p\mathbf{g}-6\pi a\mu(\mathbf{V}-\mathbf{u}), \tag{1}$$

where g is the gravity, μ the surrounding fluid viscosity, m_p is the particle's mass, a its radius, $\mathbf{V}$ its velocity, and $\mathbf{u}$ the Eulerian velocity at the particle position. In the above equation the drag force is assumed to be linear (Stokes drag). The Stokes drag assumption is valid when the particle's Reynolds number is less than one:

$$\frac{|\mathbf{u}-\mathbf{V}|d}{\nu}<1, \tag{2}$$

where d is the particle's diameter. Equation (1) can be rewritten as

$$\frac{d\mathbf{V}}{dt}=\frac{1}{\tau_a}(\mathbf{u}-\mathbf{V}+\mathbf{V}_d), \tag{3}$$

where

$$\tau_a=\frac{m_p}{6\pi a\mu} \tag{4}$$

is the aerodynamics response time and

$$\mathbf{V}_d=\tau_a\mathbf{g} \tag{5}$$

the Stokes terminal fall velocity in still fluid or particle drift velocity. Condition (2) can be met by choosing τ_a small enough. For sake of convenience we introduce two nondimensional parameters, the drift parameter defined as the ratio of the particle's drift velocity to the turbulence velocity fluctuation rms value u':

$$\gamma=\frac{V_d}{u'}=\frac{\tau_a g}{u'} \tag{6}$$

and the Stokes number defined as the ratio of the particle's inertial time to the turbulence characteristic time:

$$\mathrm{St}=\frac{\tau_a u'}{L}, \tag{7}$$

where L is the turbulence integral length-scale. For sake of comparison with literature we also introduce $\gamma_\eta=V_d/v_\eta$ and $\mathrm{St}_\eta=\tau_a v_\eta/\eta$ where v_η and η are, respectively, the Kolmogorov velocity and length scales.

C. Lagrangian method and KS

The fluid particle positions $\mathbf{X}(t)$ are governed by the equation

$$\frac{d\mathbf{X}(t)}{dt}=\mathbf{u}(\mathbf{X},t), \tag{8}$$

where $\mathbf{u}(\mathbf{X},t)$ is the Eulerian velocity field given by the Navier-Stokes equations. For particles with mass an additional equation for the Lagrangian velocity $\mathbf{V}(t)$ is needed

$$\frac{d\mathbf{X}(t)}{dt}=\mathbf{V}(t),$$

$$\frac{d\mathbf{V}(t)}{dt}=\mathcal{F}(\mathbf{V}(t),\mathbf{u}(\mathbf{X},t)). \tag{9}$$

In this paper the equation for the Lagrangian velocity is given by Eq. (3). Solving Eqs. (8) or (9) requires $\mathbf{u}$ at $\mathbf{X}$ and t, that is solving the Navier-Stokes equations at a given time and position. The straightforward method is to use direct numerical simulation (DNS) to solve Navier-Stokes equations as with DNS no approximation of the governing equations is needed. But in order to ensure sufficient spatial and temporal resolution requirements adequately, and numerical stability, it is necessary to restrict the Reynolds number on the simulation [7].

Another approach is to accept some degree of modelling in the Eulerian velocity field as long as it does not affect the Lagrangian results. Kinematic simulation (KS) were introduced as a unified Lagrangian model for one- and two-particle turbulent diffusion where incompressibility is enforced by construction in the generation of every particle trajectory. Further reference on KS can be found in [2,8,9]. More than two particles can of course also be studied with KS (e.g., [4,10]).

The velocity field is a continuous function of space and time, rather than a fixed grid of discrete values. The function (using sines and cosines) can be computed fast enough so that it is possible to compute trajectories of particles accurately, by calculating exactly the velocity at each point of the trajectory. This has to be contrasted with Eulerian grid based methods, where this has to be estimated by interpolation, which can lead to serious errors, particularly in relative diffusion. Hence, with KS, turbulence statistics can be achieved for high Reynolds numbers. KS velocity fields are Gaussian but not Dirac-correlated in time [2,8], and this non-Markovianity is an essential ingredient in KS. Comparisons of DNS and laboratory experiments of two-particle statistics in stationary isotropic turbulence have shown good agreement with KS (e.g., [9,11–13]).

D. KS velocity field

As in [3,4] our 3D KS velocity field is given as a sum of N random Fourier modes, i.e.,

$$\mathbf{u}(\mathbf{x},t)=\sum_{n=1}^{N}(\mathbf{a_n}\times\hat{\mathbf{k}}_n)\cos(\mathbf{k}_n\cdot\mathbf{x}+\omega_n t)+(\mathbf{b_n}\times\hat{\mathbf{k}}_n)\sin(\mathbf{k}_n\cdot\mathbf{x}+\omega_n t).$$

$\hat{\mathbf{k}}_n$ defined as $\hat{\mathbf{k}}_n=\mathbf{k}_n/|\mathbf{k}_n|$ is a random unit vector. $\mathbf{a}_n$ and $\mathbf{b}_n$ are random and uncorrelated vectors with their amplitudes

being chosen according to a prescribed power law energy spectrum $E(k)$, i.e.,

$$|\mathbf{a}_n \times \hat{\mathbf{k}}_n|^2 = |\mathbf{b}_n \times \hat{\mathbf{k}}_n|^2 = 2E(k_n)\Delta k_n \tag{10}$$

and

$$E(k) = \frac{u_0^2}{k_1}\left(\frac{k}{k_1}\right)^{-5/3} \text{ for } k_1 \leqslant k \leqslant k_N,$$

$$E(k) = 0, \text{ otherwise}. \tag{11}$$

Typical turbulence parameters we vary are the integral length scale

$$L = \frac{3\pi}{4}\frac{\int_{k_1}^{k_N} E(k)k^{-1}dk}{\int_{k_1}^{k_N} E(k)dk}, \tag{12}$$

the turbulent velocity fluctuation intensity

$$u' = \sqrt{\frac{2}{3}\int E(k)dk},$$

and the Kolmogorov length scale, defined here as

$$\eta = \frac{2\pi}{k_N}.$$

The characteristic time associated to this scale is

$$\tau_\eta = \frac{L}{u'}\left(\frac{\eta}{L}\right)^{2/3}.$$

The distribution of the wave number is geometric, i.e.,

$$k_n = k_1\left(\frac{k_N}{k_1}\right)^{(n-1)/(N-1)}. \tag{13}$$

It is also possible to introduce a frequency ω_n that determines the unsteadiness associated with the nth wave mode. Malik and Vassilicos [9] chose it to be proportional to the eddy-turnover time of the nth wavemode, i.e.,

$$\omega_n = \lambda\sqrt{k_n{}^3 E(k)}, \tag{14}$$

where λ is the unsteadiness parameter and may be expected to be of the order of 1. It has been shown in 3D isotropic KS [9] that for two-particle diffusion most statistical properties are insensitive to the unsteadiness parameter's value provided that it rests in the range $0 \leqslant \lambda \leqslant 1$. Nicolleau and El-Maihy [4] also concluded that, in that range of values, λ has no effect on the fractal dimension of a cloud of fluid particles. In accordance with these results we do not add any unsteadiness term to the KS.

Fluid-particles' trajectories $\mathbf{X}(t)$ are obtained by integrating

$$\frac{d\mathbf{X}}{dt} = \mathbf{u}(\mathbf{X},t) \tag{15}$$

using a 4th-order predictor corrector method (Adams-Bashforth-Moulton) in which a 4th-order Runge-Kutta scheme is used to compute the first three points needed to initialize the method. Other schemes have been investigated for sake of comparison, the Adams-Bashforth-Moulton scheme gave the best performance in terms of error growth, stability and computing time. In each realization the initial position of one particle and the orientation of the pair are chosen randomly.

For each run of the simulation, the statistical quantities are obtained by taking the ensemble average over many realizations; most of the results in this paper are computed from 2000 realizations of the velocity field. It is important to take the average of many realizations (rather than allowing the simulation to run for a long time) because in any realization considerable anisotropy is present due to the random choice of the wave vectors and initial positions of the particle.

For each realization of the velocity field, the trajectories for the two particles were computed simultaneously. The initial vector separation between the two particles was

$$\mathbf{\Delta}_0 = \Delta_0\begin{pmatrix} \frac{1}{\sqrt{3}} \\ \frac{1}{\sqrt{3}} \\ \frac{1}{\sqrt{3}} \end{pmatrix}, \tag{16}$$

where Δ_0 is an input parameter. The time step is determined by the need to track the motion of the fluid elements down to the smallest scales. It must be smaller than both the smallest eddy turnover time and the time that a typical fluid particle would take on average to move by a Kolmogorov length scale. In practice, we validate our time step by observing the ballistic or t^2 regime for two-particle diffusion. Decreasing further the time scale would not improve the resolution of this regime but would increase the total computational time.

For sake of simplicity we set the initial time when the particles are released to 0.

II. PRELIMINARY RESULTS FOR FLUID PARTICLES IN 3D

A. PDF of fluid-particle pairs

First, we complete the results of [11] to 3D KS in order to get a benchmark for the heavy-particle dispersion to be compared with. We study the diffusion of one and two fluid particles in isotropic turbulence by varying the initial separations. The different cases studied here correspond to $u'=1$, $L=1$, $\eta=2\pi\times10^{-3}$, $\tau_d=L/u'=1$, and $k_N/k_1=1000$ that is $\mathrm{Re}=(k_N/k_1)^{4/3}=10000$. The different initial separations considered are

$$\frac{\Delta_0}{\eta} = 0.01, 0.1, 0.5, 1, 4, \text{ and } 16. \tag{17}$$

We briefly generalize the results found in [11] from 2D KS to 3D KS. We define the two-particle separation as

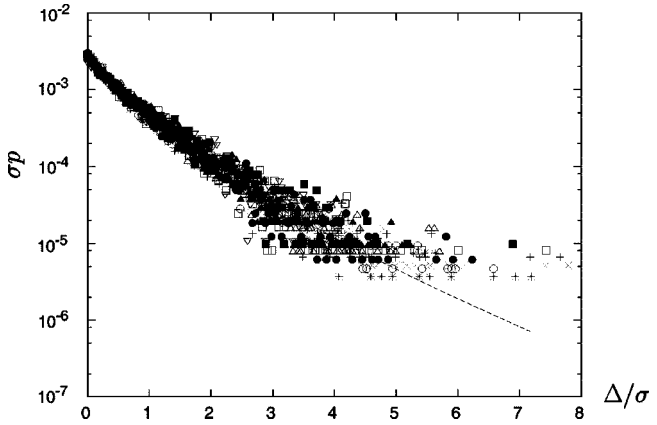

FIG. 1. σp as a function of Δ/σ for $\Delta_0=0.1\eta$: (+) $t=2.5(L/u')$, (×) $3(L/u')$, (*) $3.5(L/u')$, (□) $4(L/u')$ and (■) $4.5(L/u')$; $\Delta_0=\eta$: (○) $t=2.5(L/u')$, (●) $3(L/u')$, (△) $3.5(L/u')$, (▲) $4(L/u')$ and (▽) $4.5(L/u')$. The fitting curve is $y=0.003\exp(-2.1x^{0.7})$.

$$\Delta(t) = |\mathbf{x}_2(t) - \mathbf{x}_1(t)|, \tag{18}$$

where $\mathbf{x}_1(t)$ and $\mathbf{x}_2(t)$ are the position vectors of each of the two particles, and the root mean square of the two particles' separation as

$$\sigma(t) = \langle \Delta^2(t) \rangle^{1/2}.$$

The pair's initial separation is given at $t=0$ by

$$\Delta_0 = |\mathbf{x}_2(0) - \mathbf{x}_1(0)|.$$

The probability density functions (pdf) of Δ predicted by [14–16] are all of the form

$$p(\Delta,t) \sim \sigma^{-1} \exp\left\{ -\alpha \left(\frac{\Delta}{\sigma} \right)^{\beta} \right\} \tag{19}$$

with different values of the dimensionless parameters α and β. Richardson's prediction for the exponent β is $\beta=2/3$, Batchelor's $\beta=2$ and Kraichnan's $\beta=4/3$ (see [17]).

In Fig. 1 we plot the rescaled pair diffusion pdf σp as a function of Δ/σ for two different initial separations: $\Delta_0=0.1\eta$ and η. All the data collapse on a curve well approximated by

$$p(\Delta,t) = \frac{0.003}{\sigma} \exp\left\{ -2.1 \left(\frac{\Delta}{\sigma} \right)^{0.7} \right\}. \tag{20}$$

These values of α and β are consistent with the finding of [11] in 2D KS that is $\alpha \simeq 2.6$ and $\beta \simeq 0.6$. So that 3D KS results seem slightly closer to the prediction of Richardson than 2D KS results. We have checked that these values are not function of the Reynolds number at least in the range $50 \leqslant k_N/k_1 \leqslant 1000$.

In Fig. 2 we plot the normalized correlation function for the pair separation:

$$\frac{R(t,\tau)}{R(t,0)} = \frac{\langle \Delta(t)\Delta(t+\tau) \rangle}{\sigma^2(t)} \tag{21}$$

as a function of τ/t, at different times and for the two cases $\Delta_0/\eta=0.1$ and 1. We find that at a time t after its release the pair separation keeps memory of its previous values for a time lag $\tau \simeq 0.6t$. Our results are consistent with the results found in 2D KS [11] and even closer to the experimental results of [17].

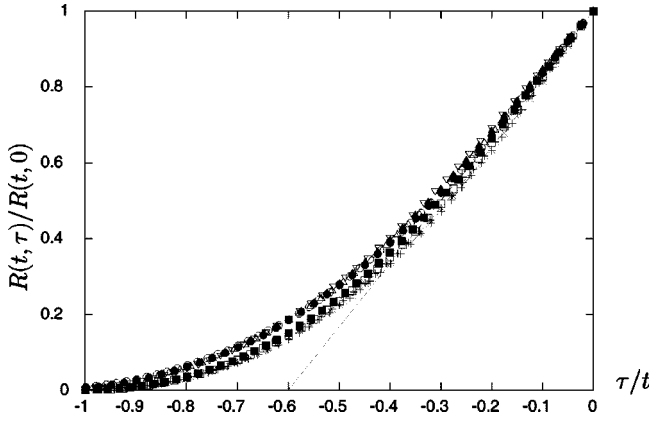

FIG. 2. $R(t,\tau)/R(t,0)$ as a function of τ/t for $\Delta_0/\eta=0.1$: (+) $t=2.5(L/u')$, (×) $3(L/u')$, (*) $3.5(L/u')$, (□) $4(L/u')$ and (■) $t=4.5(L/u')$; for $\Delta_0/\eta=1$: (○): $2.5(L/u')$, (●) $3(L/u')$, (△) $3.5(L/u')$ (▲) $4(L/u')$ and (▽) $t=4.5(L/u')$.

B. Two-particle diffusion and the locality-in-scale hypothesis

Another quantity of interest is the two-particle mean diffusivity defined as

$$\frac{d}{dt}\langle \Delta^2(t) \rangle. \tag{22}$$

This quantity was studied in [14] as a function of $\langle \Delta^2(t) \rangle$. The locality-in-scale hypothesis, stated as "in the inertial range, the dominant contribution to turbulent diffusivity $(d/dt)/\overline{\Delta^2}(t)$ at time t comes from 'eddies' of size $(\overline{\Delta^2})^{1/2}(t)$" and called locality assumption in [2], leads to

$$\frac{d\langle \Delta^2 \rangle}{dt} \sim \langle \Delta^2 \rangle^{2/3}, \tag{23}$$

which implies that

$$\langle \Delta^2 \rangle \simeq G\epsilon t^3 \tag{24}$$

a relation known as the Richardson t^3 law (24). In this paper, in agreement with [18], we prefer to work directly on Eq. (23), as it was shown to give better scalings and enable better validations of the locality-in-scale hypothesis [3].

In Fig. 3 we plot the normalized diffusivity $(d/dt) \times \langle \Delta^2(t) \rangle (1/u'\eta)$ as a function of Δ^2/η^2 for different separations (17). All the curves collapse on a single one. The line of slope 2/3 in this figure indicates the range of validity of relation (23). For small separations $\Delta/\eta < 1$ a slope 1 indicates an exponential law:

$$\langle \Delta^2 \rangle \sim e^{Ct}.$$

These different regimes are discussed in [3]. It is worth noticing that as in [3] the exponential regime exists only for very small separations $\Delta_0/\eta \leqslant 0.01$ and C is a function of Δ_0. We also define Γ as

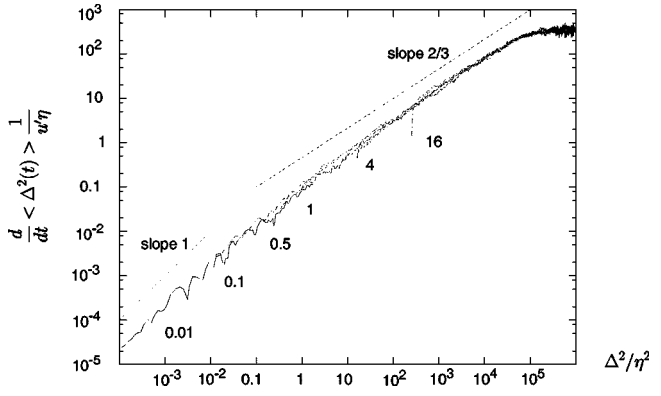

FIG. 3. Normalized diffusivity $(d/dt)\langle\Delta^2(t)\rangle(1/u'\eta)$ as a function of Δ^2/η^2 for $L/\eta=1000$ and different initial separations: as indicated from left to right $\Delta_0/\eta=0.01$, 0.1, 0.5, 1, 4, and 16.

$$\Gamma = \frac{\frac{1}{u'\eta}\frac{d\sigma^2}{dt}}{\left(\frac{\eta}{L}\right)^{1/3}\left(\frac{\Delta}{\eta}\right)^{4/3}}. \tag{25}$$

Γ is the best indicator of the locality-in-scale hypothesis. A constant value of Γ indicates the range of validity for this hypothesis. Note that for sake of comparison we use here the definition of Γ introduced in [3] (called β therein) though in the present paper η/L is not varied.

III. KINEMATIC SIMULATION FOR HEAVY PARTICLE DISPERSION

The problem of tracking a solid particle in a velocity field $\mathbf{u}(\mathbf{x},t)$ is solved by integrating

$$\frac{d\mathbf{X}(t)}{dt} = \mathbf{V}(t), \tag{26}$$

where $\mathbf{V}(t)$ is given by the simplified equation for the Lagrangian velocity for heavy particles (3). $\mathbf{u}(\mathbf{x},t)$ is the velocity field generated by kinematic simulation.

The initial condition is

$$\mathbf{V}(t=0) = \mathbf{u}(\mathbf{X}(t=0),0) + \mathbf{V}_d \tag{27}$$

and the initial position of the particle is chosen randomly in each realisation. Other initial conditions have been proposed; see, e.g., [5]. Here, we follow [19] choosing the simplest initial condition as possible.

We generalize definition (18) and the definition of the diffusivity (22) to a pair of heavy particles. We are now looking for laws in the form of

$$\frac{d\langle\Delta^2\rangle}{dt} \sim \langle\Delta^2\rangle^{\alpha}. \tag{28}$$

KS allow us to simulate many cases with different values for γ and the Stokes number. The different cases are reported in Tables I and II. The criteria for our equations to be valid is that the particle's Reynolds number is smaller than 1. With the parameters in Tables I and II such Reynolds numbers can be achieved for water droplets in air when $d<16\times10^{-6}$ m or iron ore in air when $d<10\times10^{-6}$ m (we took these examples from [20]).

TABLE I. Different initial separations and Stokes numbers used for heavy-particle simulations ($\gamma=0$). Turbulence parameters are $u'=1$, $L=0.97$, and $\eta=2\pi\times10^{-3}$; that is, $\tau_d=L/u'=0.97$ and $k_N/k_1=1000$ or $\mathrm{Re}=(k_N/k_1)^{4/3}=10000$.

Case	$\frac{\Delta_0}{\eta}$	St	St_η
IA1	0.1	1	0.1
IB2	0.1	0.8	0.08
IB3	0.1	0.6	0.06
IB4	0.1	0.4	0.04
IB5	0.1	0.2	0.02
IB6	0.1	0.1	0.01
IA2	0.5	1	0.1
IA3	1	1	0.1
IC1	4	1	0.1
IC2	4	0.8	0.08
IC3	4	0.6	0.06
IC4	4	0.4	0.04
IC5	4	0.2	0.02
IC6	4	0.1	0.01

In Fig. 4 the inertia parameter St is held constant and the fall velocity parameter ($\gamma=Vd/u'$) varied. The figure shows that for small fall velocities the particles remain suspended and show no preferred direction whereas as γ is increased the particles drift in the direction of the body force.

IV. EFFECT OF PARTICLE INERTIA ONLY ($\gamma=0$) ON TWO-PARTICLE DISPERSION

In this section we investigate the dependence of the relative dispersion and diffusivity of two heavy particles on the Stokes number, St, in the absence of gravity ($\gamma=0$). In the absence of gravity a particle disperses in an isotropic turbulence field and the departure from the fluid particle paths is due to the inertial effect only. In this instance, the dispersion is totally isotropic so that the subscripts on the velocity vectors can be dropped.

In Fig. 5 we plot the two-particle dispersion, $\langle\Delta^2\rangle/\eta^2$, as a function of t/τ_η for (a) $\Delta_0=0.1\eta$ and (b) $\Delta_0=4\eta$ and for different Stokes numbers, namely, St=0.05, 0.2, 0.4, 0.8, and 1. Figure 6 shows, for the same cases (a) and (b), a log-log plot of the normalized diffusivity as a function of the normalized mean square displacement between the two particles. For sake of comparison the same curves are obtained for a fluid-particle pair diffusion.

The particles' dispersion can be divided into four regimes; the first regime corresponds to small times; that is small separations between the two particles. In this regime the particles move approximately in straight lines:

$$\langle\Delta^2\rangle \simeq \Delta_0^2 + (\Delta V_0)^2 t^2 \tag{29}$$

or in terms of diffusivity as can be seen in Fig. 6:

TABLE II. Different KS used for the study of heavy-particles in different gravity fields.

u'	L	η	$\tau_d=\frac{L}{u'}$	$\frac{k_N}{k_1}$	$\mathrm{Re}=\left(\frac{k_N}{k_1}\right)^{4/3}$	$\frac{\Delta_0}{\eta}$	γ	γ_η	St	St_η
1	0.97	$2\pi\times10^{-3}$	0.97	1000	10000	0.1	0.2	2	0.02	0.002
1	0.97	$2\pi\times10^{-3}$	0.97	1000	10000	0.1	0.6	6	0.02	0.002
1	0.97	$2\pi\times10^{-3}$	0.97	1000	10000	0.1	1	10	0.02	0.002
1	0.97	$2\pi\times10^{-3}$	0.97	1000	10000	0.1	2	20	0.02	0.002
1	0.97	$2\pi\times10^{-3}$	0.97	1000	10000	0.1	4	40	0.02	0.002
1	0.97	$2\pi\times10^{-3}$	0.97	1000	10000	4	0.2	2	0.02	0.002
1	0.97	$2\pi\times10^{-3}$	0.97	1000	10000	4	0.6	6	0.02	0.002
1	0.97	$2\pi\times10^{-3}$	0.97	1000	10000	4	1	10	0.02	0.002
1	0.97	$2\pi\times10^{-3}$	0.97	1000	10000	4	2	20	0.02	0.002
1	0.97	$2\pi\times10^{-3}$	0.97	1000	10000	4	4	40	0.02	0.002

$$\frac{d}{dt}\langle\Delta^2\rangle \sim \langle\Delta^2\rangle^{1/2}.$$

The length of this regime depends on the particle inertia. As shown in Fig. 6, this regime's duration increases with the particle inertia, this can be attributed to the fact that particles with higher inertia take longer times to forget their initial conditions. This is clear in the curves corresponding to St $\simeq 1$ in which the slope of the diffusivity is $1/2$ for nearly 2 decades.

In Fig. 7(a) we plot τ_{set}, the time duration of this first regime as a function of the Stokes number. This time of settlement increases linearly with the Stokes number:

$$\frac{\tau_{set}}{\tau_\eta} = \mathcal{T}\,\mathrm{St} + \mathcal{B}. \tag{30}$$

This linear relation is not compatible with the locality-in-scale hypothesis. Indeed, Morel and Larchevêque's approach [18] can be generalized to include a dependence on the inertia parameter τ_a for the diffusivity:

$$\frac{d}{dt}\langle\Delta^2\rangle = f(\sigma, E(\sigma), \tau_a)$$

or in terms of characteristic times

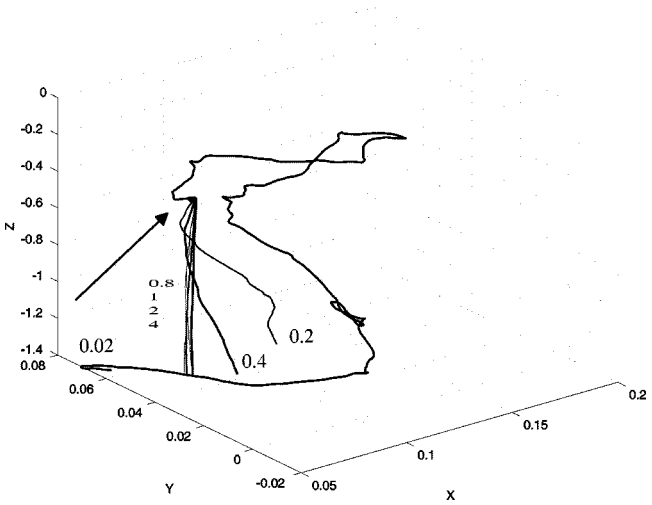

FIG. 4. Example of heavy particle trajectories for St=0.02 and different values of γ: γ=0.005, 0.01, 0.05, 0.1, 0.5, 1, and 4. The arrow points at the location where the particles are released.

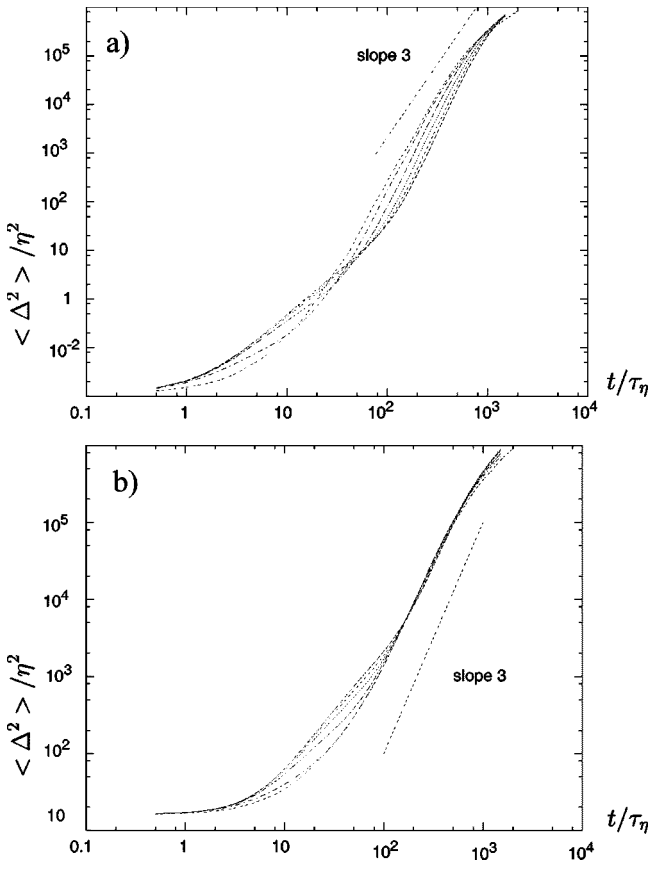

FIG. 5. Two-particle normalized diffusion $\langle\Delta^2\rangle/\eta^2$ as a function of t/τ_η, effect of inertia only (γ=0), (a) $\Delta_0=0.1\eta$ and (b) $\Delta_0=4\eta$. Cases are taken from Table I; in each plot from top to bottom St =1, 0.8, 0.6, 0.4, 0.2, 0.05 and fluid particle.

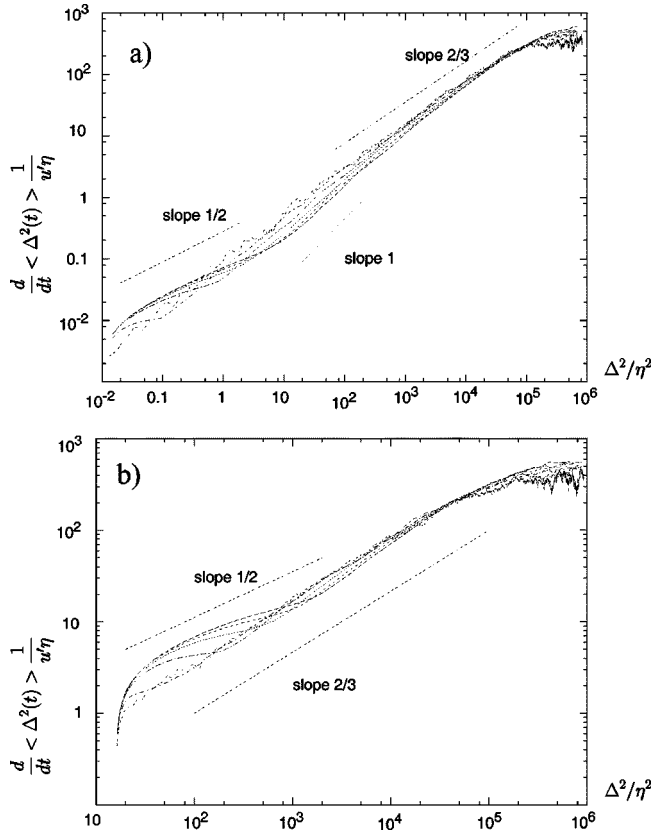

FIG. 6. Two-particle normalised diffusivity $(d/dt)\langle\Delta^2\rangle/u'\eta$ as a function of $\langle\Delta^2\rangle/\eta^2$, effect of inertia only ($\gamma=0$), (a) $\Delta_0=0.1\eta$ and (b) $\Delta_0=4\eta$. Cases are taken from Table I; in each plot from top to bottom St=1, 0.8, 0.6, 0.4, 0.2, 0.05 and fluid particle.

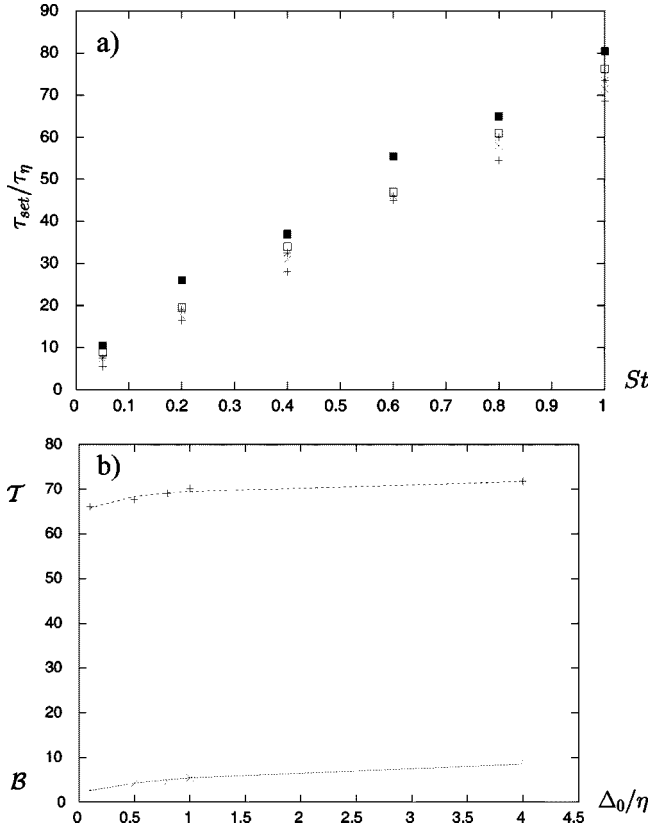

FIG. 7. Effect of inertia ($\gamma=0$) on the nondimensional time τ_{set}/τ_η needed for the two particles to leave the first regime. (a) τ_{set}/τ_η as a function of St for $\Delta_0=0.1\eta$ (+), 0.5η (×), 0.8η (*), 1η (□), and 4η (■). (b) Linear coefficients $\mathcal{T}$ (+) and $\mathcal{B}$ (×) from Eq. (30) as functions of Δ_0/η. Interpolating curves are respectively $\mathcal{T}=1.62\ln(\Delta_0/\eta)+69.52$ and $\mathcal{B}=1.72\ln(\Delta_0/\eta)+5.9$.

$$\frac{d}{dt}\langle\Delta^2\rangle = f(\tau_\sigma, \epsilon, \tau_a),$$

where τ_σ is the characteristic time associated to eddies of size σ. There are therefore two competing regimes: the inertia dominated regime when $\tau_a > \tau_\sigma$ and the turbulence dominated regime when the pair separation is large enough: $\tau_\sigma > \tau_a$.

The criteria for the end of the inertia dominated regime is therefore

$$\tau_\sigma \simeq \tau_a. \tag{31}$$

That is, using $\tau_\sigma=(L/u')(\sigma/L)^{2/3}$ for an eddy of size σ, when

$$\sigma = \sigma_{set} \simeq \tau_a^{3/2}\left(\frac{u'}{L}\right)^{3/2} L = \mathrm{St}^{3/2} L.$$

But by definition, until τ_{set}, σ is governed by Eq. (29). So that

$$\sigma_{set} \simeq \Delta V_0 \tau_{set}$$

and when σ_{set} is reached:

$$\Delta V_0 \tau_{set} \simeq \mathrm{St}^{3/2} L,$$

that is

$$\tau_{set} \simeq \mathrm{St}^{3/2}\frac{L}{\Delta V_0}, \tag{32}$$

whereas we find a linear dependence on the Stokes number which means that particle pairs are actually influenced by eddies of characteristic time $\sqrt{\mathrm{St}}$ times smaller than what a locality-in-scale hypothesis would predict. Therefore, we can conclude that whatever the initial separation, there is no locality in scale when $t \leqslant \tau_{set}$. Later on, we will also conclude analyzing the subsequent pair separation regime that inertia tends to invalidate the locality in scale hypothesis for $\Delta_0 < \eta$ at all times.

The time of settlement varies also slightly with the initial separation as shown in Fig. 7(b) where we plot $\mathcal{T}$ and $\mathcal{B}$ from Eq. (30) as functions of Δ_0/η. So that the overall effect is

$$\frac{\tau_{set}}{\tau_\eta} = \left\{1.62\ln\left(\frac{\Delta_0}{\eta}\right) + 69.52\right\}\mathrm{St} + 1.72\ln\left(\frac{\Delta_0}{\eta}\right) + 5.9. \tag{33}$$

The validity of (29) corresponds to a region of almost constant velocity gradients. For small initial separations, the constant $\mathcal{B}$ in (30) is or the order of unity. This can be explained as for small inertia $\mathrm{St} \ll 1$ the particles stay in regions of constant velocity gradients during a time that scales with

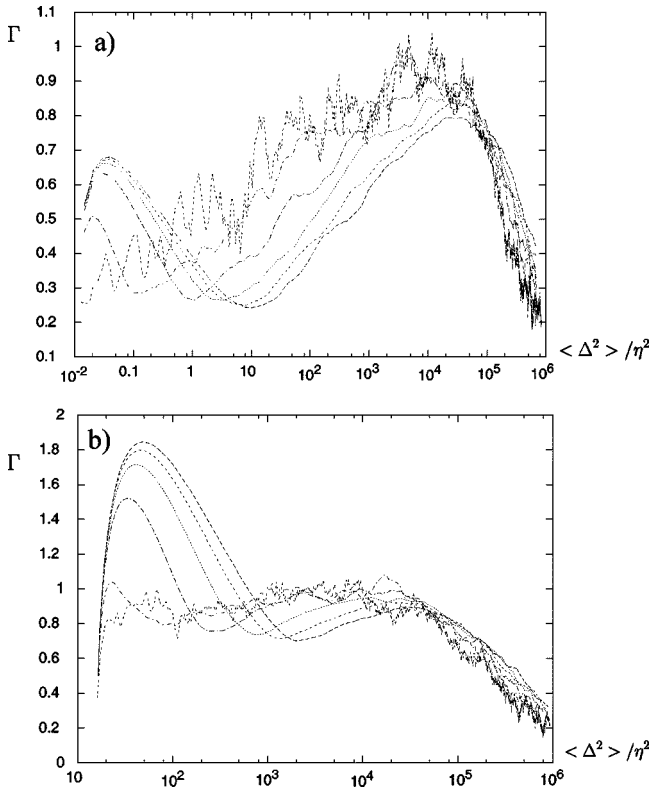

FIG. 8. Effect of inertia ($\gamma=0$) on the value of Γ as a function of $\langle\Delta^2\rangle/\eta^2$ for $\Delta_0=0.1\eta$ (a) and $\Delta_0=4\eta$ (b). On each plot the different curves are St=1, 0.8, 0.6, 0.4, 0.2, 0.05 and fluid-particle diffusion.

the Kolmogorov time scale. This is the limit from heavy particles to fluid particles.

By contrast, when $\mathrm{St}\gg 1$ the dispersion is characterized by the memory of the initial conditions, τ_{set} then scales as the characteristic time of the particle (i.e., τ_a). In this case, τ_{set}/τ_η is proportional to $\mathrm{St}\tau_L/\tau_\eta$ which in turn is proportional to $\mathrm{St}(L/\eta)^{2/3}$. This is supported by the values of $\mathcal{T}$ in (30) which are of the order $(L/\eta)^{2/3}=100$ for the cases of Fig. 7(b) $(L/\eta=10^3)$.

The second regime is an exponential law characterized, as can be seen from the diffusivity plots, by

$$\frac{d}{dt}\langle\Delta^2\rangle \sim \langle\Delta^2\rangle$$

suggesting that $\langle\Delta^2\rangle \sim e^{t/\tau_\eta}$. It is a transition between the first regime and the Richardson regime. As noted previously this regime can only be observed for very small initial separations $\Delta_0/\eta \leqslant 0.01$. However, it seems that such a law appears in Fig. 6 for $\Delta_0/\eta=0.1$ when St increases but at a delayed position when $10<(\Delta/\eta)^2<100$.

The third regime corresponds to Richardson's law where the pair dispersion is close to the prediction of the locality-in-scale hypothesis (23) as indicated by the line of 2/3 slope in Fig. 6(a). As shown by [3], the best way to assess Richardson's law is to measure Γ [see Eq. (25)].

In Fig. 8 we plot Γ as a function of $\langle\Delta^2\rangle/\eta^2$ for $\Delta_0=0.1\eta$ (a) and 4η (b) and for different Stokes numbers.

In agreement with the result of [3] for $\Delta_0=4\eta$, Γ is constant for the fluid particle over the range of scales $50<\sigma/\eta<1000$. The effect of inertia is to decrease this range which disappears completely for $\mathrm{St}>1$. As can be seen from Eq. (32) for $\mathrm{St}\geqslant 1$, $\tau_{set}\geqslant L/u'$ and there is no more range for the locality in scale to be observed.

For small initial separations, $\Delta_0/\eta<1$, Nicolleau and Yu [3] found that Γ was not constant thus invalidating the hypothesis of a similarity in scales and as a consequence Richardson's t^3 law. They showed that for $\Delta_0/\eta<1$

$$\Gamma = a\ln\left(\frac{\Delta}{\eta}\right)+b, \tag{34}$$

where a and b were functions of Δ_0/η. In Fig. 8(a), the same result is found with inertia. Furthermore, the departure from the locality-in-scale hypothesis is now an increasing function of the Stokes number and we generalize formula (34) proposed by [3] for fluid particles in order to include the effect of the Stokes number:

$$\Gamma = a(\mathrm{St})\ln\left(\frac{\Delta}{\eta}\right)+b(\mathrm{St}). \tag{35}$$

With the cases we study here, $\Delta_0/\eta=0.1$, 0.3, 0.5, 0.8, and 1, it is difficult to see any trend in the variation with the initial separation, so we consider that a and b for heavy particles, by contrast to fluid particles, are independent of Δ_0/η and only linear functions of St. Therefore, the two linear fittings we propose use all the data from the different initial separations, that is

$$a = 0.043\ \mathrm{St} + 0.06,$$

$$b = -0.65\ \mathrm{St} + 0.5. \tag{36}$$

The coefficient a is much less sensitive to the Stokes number St than the coefficient b. a is an increasing function of St, so that increasing the inertia increases the departure from Richardson's regime. By contrast, the coefficient b clearly decreases with St this is because the overall effect of increasing the inertia is to decrease the diffusivity.

The fourth regime is called the "long-time" [6] relative diffusivity. When the pair separation becomes greater than the size of the largest turbulent eddies the motion of one particle becomes independent of the other. From previous studies [21] the particle inertia was found to enhance the single-particle diffusivity and as a consequence it has the same effect for the "long-time" relative diffusivity.

V. EFFECT OF VARYING THE FALL VELOCITY PARAMETER ON TWO-PARTICLE DISPERSION

In many practical situations, the gravitational settling cannot be ignored and often plays a determining role in the particles' dispersion. For a particle suspended in isotropic turbulence yet having a steady fall velocity due to gravity, the problem retains axial symmetry in the z direction. So all the statistics will be considered in the directions perpendicular to **g** (xy plane) and in the direction parallel to **g** (z direction).

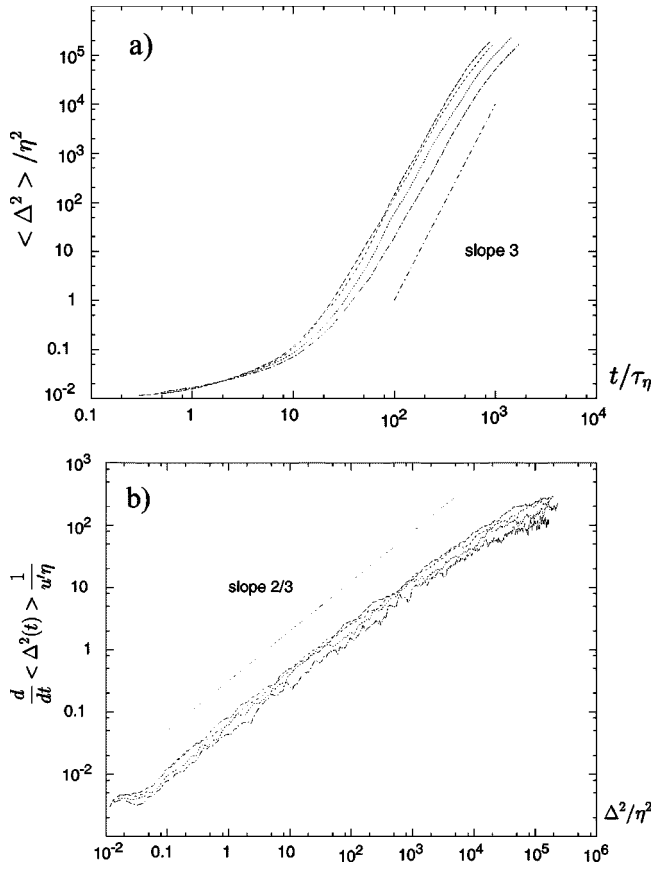

FIG. 9. Effect of gravity on the pair horizontal dispersion for $\Delta_0 = 0.1\eta$ and St=0.02. (a) Pair dispersion $\langle \Delta^2 \rangle / \eta^2$ as a function of t/τ_η. (b) Pair diffusivity $(d/dt)\langle \Delta^2 \rangle / u'\eta$ as a function of $\langle \Delta^2 \rangle / \eta^2$. Different cases are in each plot from top to bottom fluid particles, $\gamma = 0.2$, 0.6, 1, 2, and 4.

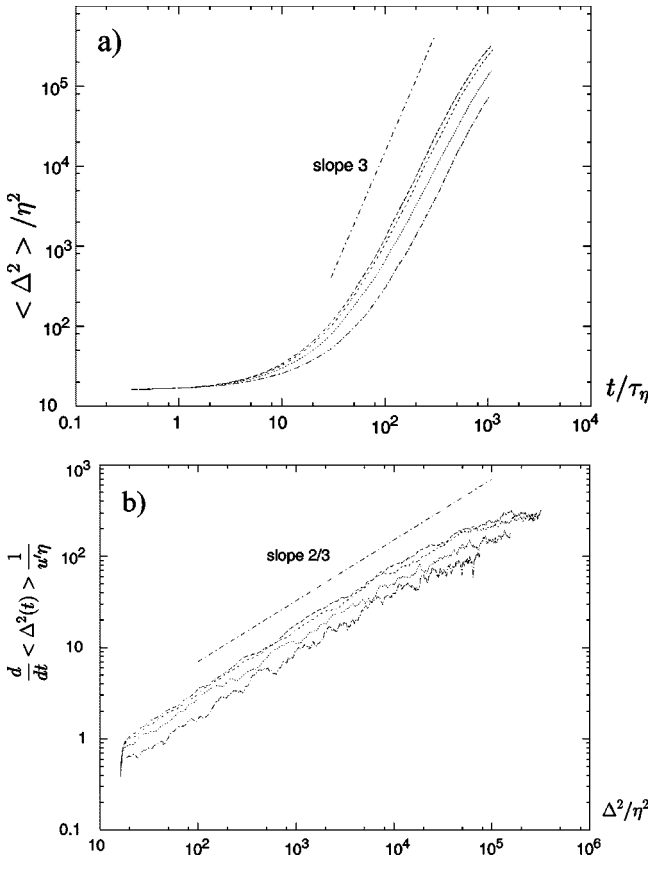

FIG. 10. Effect of gravity on the pair horizontal dispersion for $\Delta_0 = 4\eta$ and St=0.02. (a) Pair normalized diffusion $\langle \Delta^2 \rangle / \eta^2$ as a function of t/τ_η. (b) Pair normalized diffusivity $(d/dt)\langle \Delta^2 \rangle / u'\eta$ as a function of $\langle \Delta^2 \rangle / \eta^2$. Different cases are in each plot from top to bottom: fluid particles, $\gamma = 0.2$, 0.6, 1, 2, and 4.

Figure 9 shows the pair horizontal dispersion for $\Delta_0 = 0.1\eta$ and St=0.02 and different values of γ namely, $\gamma = 0.2$, 0.6, 1, 2, and 4. In Fig. 9(a) we plot the pair dispersion, $\langle \Delta_x^2 \rangle / \eta^2$, as a function of time, t/τ_η, whereas Fig. 9(b) is a log-log plot of the mean diffusivity, $(d/dt)\langle \Delta^2 \rangle / u'\eta$, as a function of the mean square displacement, $\langle \Delta^2 \rangle / \eta$. (The corresponding plots for the dispersion along the vertical axis give similar results and are not reported in this paper.)

We observe that there is no significant difference between vertical and horizontal dispersion. In terms of diffusivity we can see from Fig. 9(b) that γ has little effects on the range of scales where the locality in scale is observed but decreases the value of Γ.

Similar conclusions can be drawn for the initial condition $\Delta_0 = 4\eta$. This case is reported in Fig. 10 and we can see no effect of γ on the range where the different regimes appear but a clear decrease of the value of the diffusivity with γ.

To be more specific we can work on a relation similar to Eq. (35). Here, in the presence of gravity the coefficients a and b will be functions of γ and Δ_0 and may be anisotropic:

$$\Gamma_x = a_x(\gamma, \mathrm{St}, \Delta_0) \ln\left(\frac{\Delta}{\eta}\right) + b_x(\gamma, \mathrm{St}, \Delta_0), \tag{37}$$

$$\Gamma_z = a_z(\gamma, \mathrm{St}, \Delta_0) \ln\left(\frac{\Delta}{\eta}\right) + b_z(\gamma, \mathrm{St}, \Delta_0). \tag{38}$$

In Fig. 11 we plot Γ as a function of $\langle \Delta^2 \rangle / \eta^2$ in the horizontal direction for the different cases of Figs. 9 and 10. Similar results were found in the vertical direction. Figure 11(b) corresponds to $\Delta_0 = 4\eta$ and for this separation Richardson's law is retrieved, i.e., $a_x = a_z = 0$.

Though different in x and z directions the coefficients are of the same order of magnitude and a and b can be regarded as fairly isotropic. All the coefficients decrease when γ increases. By contrast to what was observed with inertia, introducing gravity decreases a and the departure from the locality-in-scale hypothesis. Though, as for inertia, the overall effect of gravity is to decrease b and the diffusivity.

Both coefficients are found to be linear functions of γ, and we define a_{x1}, a_{x2}, b_{x1}, b_{x2}, a_{z1}, a_{z2}, b_{z1} and b_{z2} functions of Δ_0/η only as follows:

$$a_x = a_{x1}\gamma + a_{x2}, \tag{39}$$

$$b_x = b_{x1}\gamma + b_{x2}, \tag{40}$$

$$a_z = a_{z1}\gamma + a_{z2}, \tag{41}$$

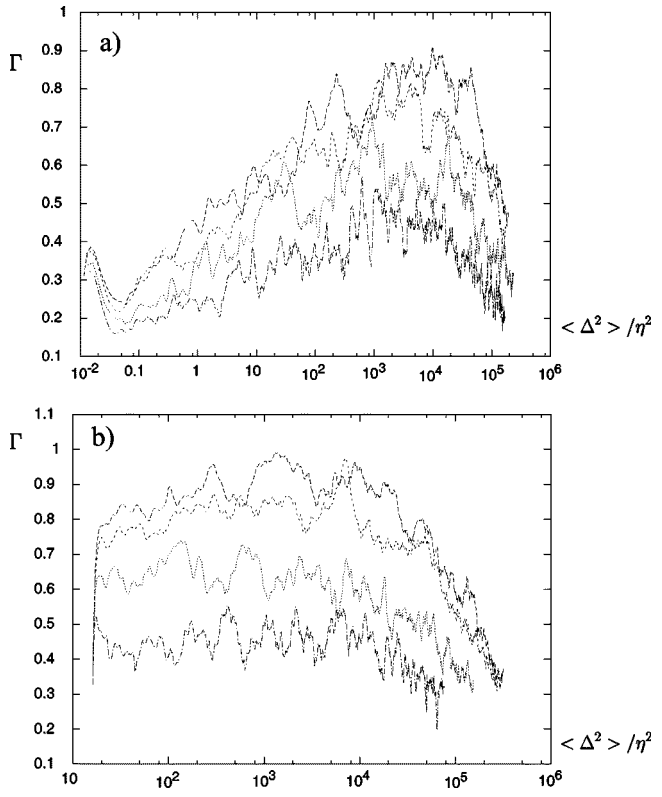

FIG. 11. Effect of gravity (St=0.02) on the value of Γ as a function of $\langle \Delta^2 \rangle / \eta^2$ in the horizontal direction for $\Delta_0 = 0.1\eta$ (a) and $\Delta_0 = 4\eta$ (b). On each plot the different curves are from top to bottom fluid particles, γ=0.2, 0.6, 1, 2, and 4.

$$b_z = b_{z1}\gamma + b_{z2}. \tag{42}$$

These different coefficients are found to be linear functions of Δ_0/η for St=0.02 and the initial separations considered here, and we find the following fitting curves:

$$a_x = \left(0.0017\frac{\Delta_0}{\eta} - 0.0068\right)\gamma - 0.015\frac{\Delta_0}{\eta} + 0.053,$$

$$b_x = \left(-0.022\frac{\Delta_0}{\eta} - 0.049\right)\gamma + 0.44e^{0.32(\Delta_0/\eta)},$$

$$a_z = \left(-0.0007\frac{\Delta_0}{\eta} - 0.0038\right)\gamma - 0.0058\frac{\Delta_0}{\eta} + 0.052,$$

$$b_z = \left(-0.0103\frac{\Delta_0}{\eta} - 0.055\right)\gamma + 0.47e^{0.22(\Delta_0/\eta)}.$$

It is worth noting that the overall decrease of the diffusivity and of b with γ is consistent with the results of [22]. In their paper the authors add a mean velocity V to the KS velocity field and found that the pair diffusion decreases with V ([22], see Fig. 4) Here, the drift velocity plays the same role.

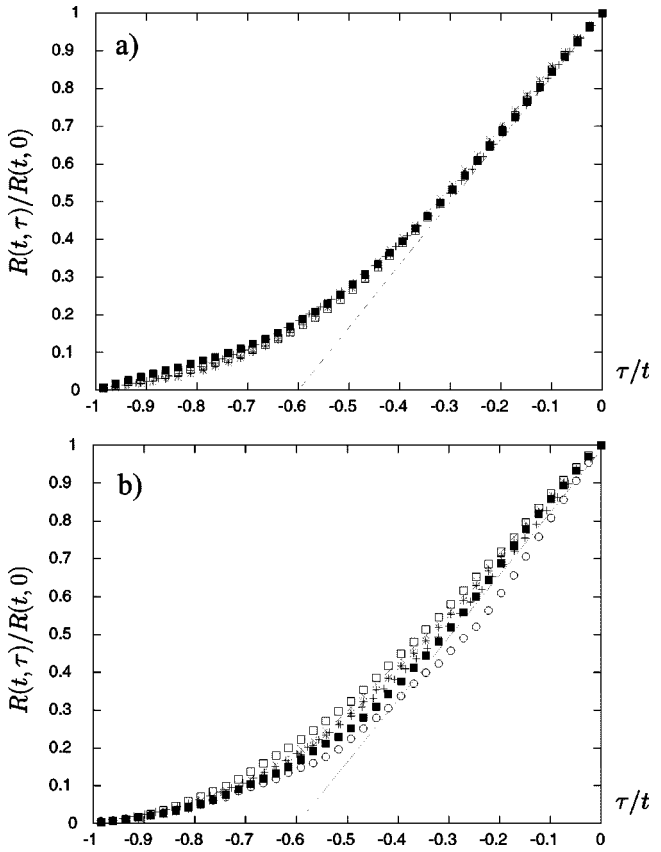

FIG. 12. $R(t,\tau)/R(t,0)$ as a function of τ/t for tu'/L=3.5 and Δ_0/η=1. (a) Effect of varying the inertia: fluid particles (+), St =0.05 (×), 0.2 (*), 0.6 (□), and 1 (■). (b) Effect of varying γ: fluid particles (+), γ=0.2 (×), 0.6 (*), 1 (□), 2 (■), and (○) 4.

VI. EFFECT OF INITIAL SEPARATION, INERTIA AND GRAVITY ON THE PARTICLE-PAIR MEMORY

The effect of the initial separation Δ_0 can be further investigated on the two-particle time-correlation function $R(t,\tau)/R(t,0)$. This later is a direct measurement of the particle-pair memory. We found that the time correlation remains isotropic when inertia and gravity are introduced so, here, we present the results for the direction x only. In Figs. 12 and 13 we study the two-particle autocorrelation in time for fluid particle, particle with inertia only and particle subjected to gravity effects for different initial separations.

(i) Figure 12 shows that when $\Delta_0 = \eta$ the inertia has no effect on the pair memory and gravity has little effect on it when $\gamma < 4$.

(ii) Figure 13 shows that compared to the fluid-particle case, the effect of inertia and gravity is to increase the pair memory dependence on the initial separation. When $\Delta_0 = 0.1\eta$ the effect is significant and the overall effect of inertia and gravity is to decrease the pair memory.

VII. EFFECT OF INERTIA AND GRAVITY ON PARTICLE PAIR PDF

In Fig. 14 we plot the rescaled two-particle diffusion pdf σp as a function of Δ/σ for two different initial separations:

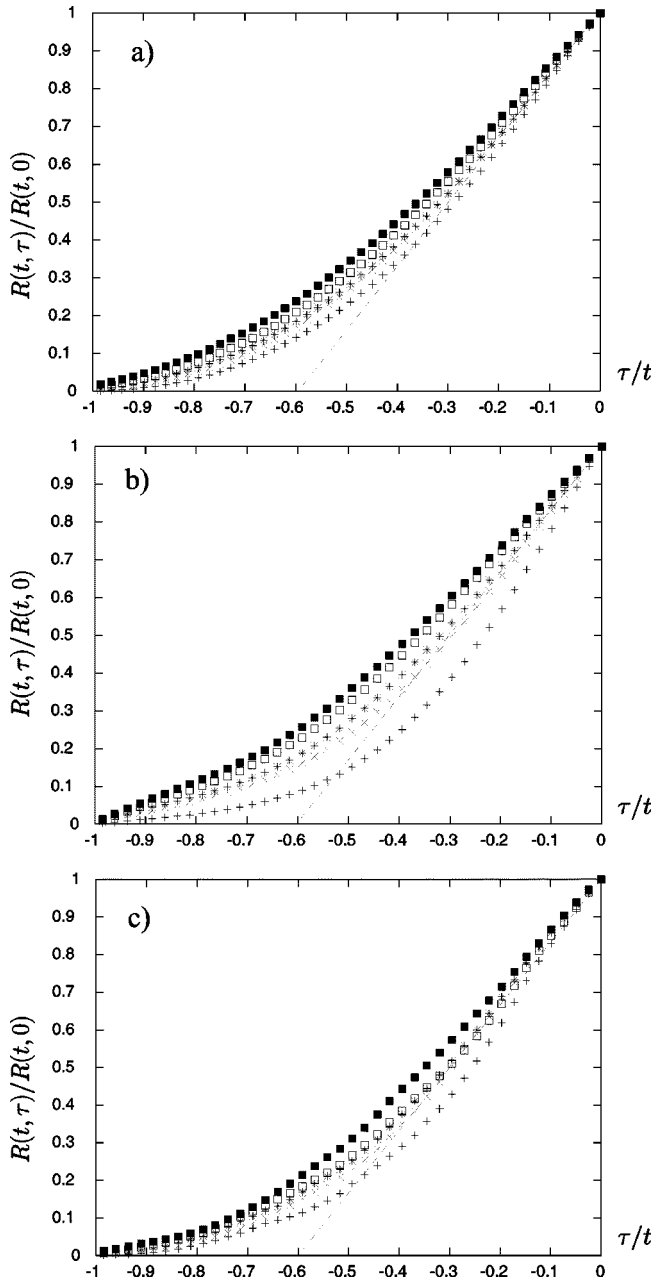

FIG. 13. Effect of initial separation on two-particle correlation function. $R(t,\tau)/R(t,0)$ as a function of τ/t for $tu'/L=3.5$ and $\Delta_0/\eta=0.1$ (+), 0.5 (×), 1 (*), 2 (□), and 4 (■). (a) Fluid particles. (b) Particle with inertia only from Table I, St=1. (c) Including gravity effects, from Table II, St=0.02 and $\gamma=2$.

$\Delta_0=0.1\eta$ and η. First, we study the effect of inertia varying St from 0.2 to 1 [Fig. 14(a)] and conclude that there is no effect of inertia on the pdf function. Then, we study the effect of γ on the dispersion along x in Fig. 14(b). (We did not observe any difference when considering the dispersion along z.) We varied the parameter γ from 0.1 to 4 and can conclude that there is no effect of γ on either the dispersion along x or z except perhaps that the results are slightly more scattered in the z direction. However, for both directions and for all γ and St values, all the data collapse on a curve well approximated by $y=0.003\exp(-2.1x^{0.7})$ that is

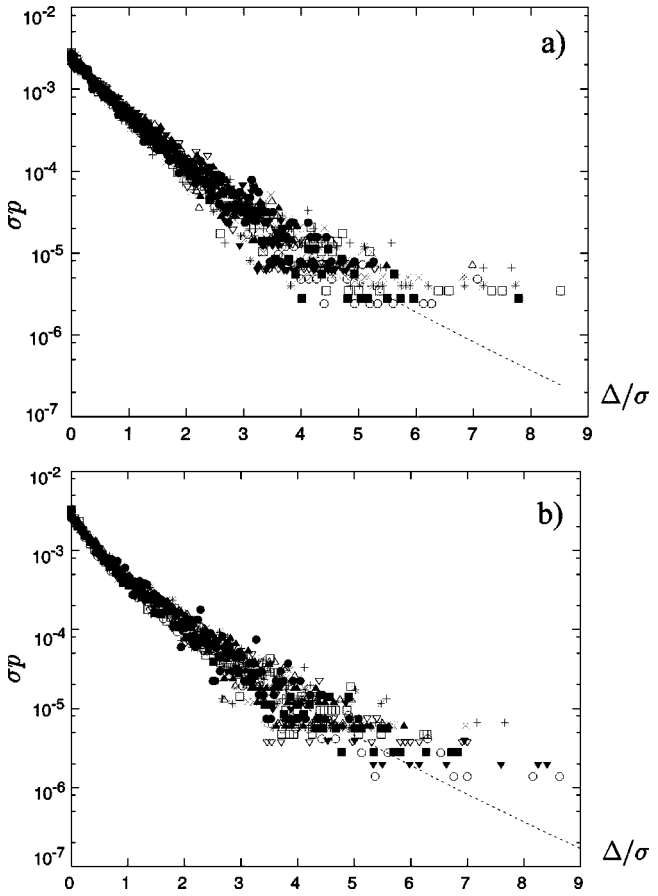

FIG. 14. σp as a function of Δ/σ for $\Delta_0/\eta=0.1$. (a) Effect of inertia: (+) fluid particles, (×) St=0.2, (*) 0.4, (□) 0.6, (■) 0.8, (○) 1; $\Delta_0/\eta=1$: (●) St=0.2, (△) 0.4, (▲) 0.6, (▽) 0.8, and (▼) 1. (b) Effect of gravity in x direction: (+) fluid particles, (×) $\gamma=0.2$, (*) 0.6, (□) 1, (■) 2, (○) 4; $\Delta_0/\eta=1$: (●) 0.2, (△) 0.6, (▲) 1, (▽) 2, and (▼) 4.

$$p(\Delta,t)=\frac{0.003}{\sigma}\exp\left\{-2.1\left(\frac{\Delta}{\sigma}\right)^{0.7}\right\},$$

which is the pdf observed for fluid particles (20). We repeated the results for two initial separations $\Delta_0=0.1\eta$ and $\Delta_0=\eta$ to make sure there is no effect of the initial separation, so that we can safely conclude that the rescaled pdf is not affected by either inertia or gravity.

VIII. CONCLUSIONS

In this paper we generalize Nicolleau and Yu's [3] approach of the diffusivity to particles with inertia and study the locality-in-scale hypothesis and departure from Richardson's regime as functions of the Stokes number and the gravity parameter γ.

In the presence of inertia the particle pairs move in approximately straight lines during a time proportional to the Stokes number St. The inertia decreases the pair diffusivity. Furthermore, it impairs the locality-in-scale hypothesis when $\Delta_0<\eta$, but does not alter this hypothesis for $\Delta_0>\eta$.

Adding gravity to inertia does not significantly alter the pair diffusivity isotropy. The overall effect of gravity is to

decrease the diffusivity in all directions. However, it improves the validity of the locality-in-scale hypothesis when $\Delta_0 < \eta$.

We also study the pair pdf and autocorrelation in time as in [11].

The particles with initial separations $\Delta_0 < \eta$ and higher inertia remember less of their history but inertia has no effect on the pair memory when $\Delta_0 > \eta$. Gravity does not significantly alter the pair memory.

Inertia and gravity do not alter the normalized pdf, σp, which obeys the same law as for the fluid particle in all directions.

ACKNOWLEDGEMENTS

The authors want to thank Dr. Javier Davila for his useful comments which led to the final version of this paper.

[1] P. A. Durbin, J. Fluid Mech. **100**, 279 (1980).
[2] J. C. H. Fung and J. C. Vassilicos, Phys. Rev. E **57**, 1677 (1998).
[3] F. Nicolleau and G. Yu, Phys. Fluids **16**, 2309 (2004).
[4] F. Nicolleau and A. ElMaihy, J. Fluid Mech. **517**, 229 (2004).
[5] J. C. H. Fung and J. C. Vassilicos, Phys. Rev. E **68**, 046309 (2003).
[6] A. M. Reynolds, Fluid Dyn. Res. **16**, 1 (1995).
[7] J. C. H. Fung, J. C. R. Hunt, and R. J. Perkins, Proc. R. Soc. London, Ser. A **459**, 445 (2003).
[8] J. C. H. Fung, J. C. R. Hunt, N. A. Malik, and R. J. Perkins, J. Fluid Mech. **236**, 281 (1992).
[9] N. A. Malik and J. C. Vassilicos, Phys. Fluids **11**, 1572 (1999).
[10] M. A. I. Khan, A. Pumir, and J. C. Vassilicos, Phys. Rev. E **68**, 026313 (2003).
[11] F. Nicolleau and J. C. Vassilicos, Phys. Rev. Lett. **90**, 024503 (2003).
[12] F. W. Elliott and A. J. Majda, Phys. Fluids **8**, 1052 (1996).
[13] P. Flohr and J. C. Vassilicos, J. Fluid Mech. **407**, 315 (2000).
[14] L. F. Richardson, Proc. R. Soc. London, Ser. A **10**, 523 (1926).
[15] G. K. Batchelor, Proc. R. Soc. London, Ser. A **213**, 349 (1952).
[16] R. Kraichnan, Phys. Fluids **9**, 1943 (1966).
[17] M.-C. Jullien, J. Paret, and P. Tabeling, Phys. Rev. Lett. **82**, 2872 (1999).
[18] P. Morel and M. Larchevêque, J. Atmos. Sci. **31**, 2189 (1974).
[19] J. Dávila and J. C. R. Hunt, J. Fluid Mech. **440**, 117 (2001).
[20] J. C. H. Fung, Ph.D. thesis, University of Cambridge, (1990).
[21] M. W. Reeks, J. Fluid Mech. **83**, 529 (1977).
[22] J. Davila and J. C. Vassilicos, Phys. Rev. Lett. **91**, 144501 (2003).